Int J Earth Sci (Geol Rundsch) (2018) 107:251–267
https://doi.org/10.1007/s00531-017-1488-3

ORIGINAL PAPER

S-type granite generation and emplacement during a regional switch from extensional to contractional deformation (Central Iberian Zone, Iberian autochthonous domain, Variscan Orogeny)

M. F. Pereira[1] · R. Díez Fernández[2] · C. Gama[3] · M. Hofmann[4] · A. Gärtner[4] · U. Linnemann[4]

Received: 2 December 2016 / Accepted: 5 May 2017 / Published online: 19 May 2017

Abstract Zircon grains extracted from S-type granites of the Mêda-Escalhão-Penedono Massif (Central Iberian Zone, Variscan Orogen) constrain the timing of emplacement and provide information about potential magma sources. Simple and composite zircon grains from three samples of S-type granite were analyzed by LA-ICP-MS. New U–Pb data indicate that granites crystallized in the Bashkirian (318.7 ± 4.8 Ma) overlapping the proposed age range of ca. 321–317 Ma of the nearby S-type granitic rocks of the Carrazeda de Anciães, Lamego and Ucanha-Vilar massifs. The timing of emplacement of such S-type granites seems to coincide with the waning stages of activity of a D_2 extensional shear zone (i.e. Pinhel shear zone) developed in metamorphic conditions that reached partial melting and anatexis (ca. 321–317 Ma). Dykes of two-mica granites (resembling diatexite migmatite) are concordant and discordant to the compositional layering and S_2 (main) foliation of the high-grade metamorphic rocks of the Pinhel shear zone. Much of the planar fabric in these dykes was formed during magmatic crystallization and subsequent solid-state deformation. Field relationships suggest contemporaneity between the ca. 319–317 Ma old magmatism of the study area and the switch from late D_2 extensional deformation to early D_3 contractional deformation. Inherited zircon cores are well preserved in these late D_2-early D_3 S-type granite plutons. U–Pb ages of inherited zircon cores range from ca. 2576 to ca. 421 Ma. The spectra of inherited cores overlap closely the range of detrital and magmatic zircon grains displayed by the Ediacaran to Silurian metasedimentary and metaigneous rocks of the Iberian autochthonous and parautochthonous domains. This is evidence of a genetic relationship between S-type granites and the host metamorphic rocks. There is no substantial evidence for the addition of mantle-derived material in the genesis of these late D_2–early D_3 S-type granitic rocks. The εNd arrays of heterogeneous crustal anatectic melts may be just inherited from the source, probably reflecting mixing of a range of crustal materials with different ages and primary isotopic signatures. The generation of the Bashkirian S-type granites has been dominated by continental crust recycling, rather than the addition of new material from mantle sources.

Keywords Carboniferous granitic rocks · Igneous intrusion relationships · U–Pb zircon LA-ICP-MS dating · Migmatites · Crustal recycling · Variscan deformation

Electronic supplementary material The online version of this article (doi:10.1007/s00531-017-1488-3) contains supplementary material, which is available to authorized users.

✉ M. F. Pereira
mpereira@uevora.pt

1 Departamento de Geociências, ECT, Instituto D. Luiz, Universidade de Évora, Évora, Portugal

2 Departamento de Geodinámica, Instituto de Geociencias (UCM, CSIC), Universidad Complutense de Madrid, 28040 Madrid, Spain

3 Departamento de Geociências, Instituto de Ciências da Terra de Évora, ECT, Universidade de Évora, Évora, Portugal

4 Senckenberg Naturhistorische Sammlungen Dresden, Museum für Mineralogie und Geologie, Dresden, Germany

Introduction

A large extension of Carboniferous and Permian plutonic rocks crops out in the Iberian Massif (e.g., Castro et al. 2002 and references therein). In the Carboniferous, magma production occurred simultaneously with the building of the Variscan Orogen caused by the collision between Gondwana and Laurussia (Martínez Catalán et al. 1997, 2009). In the earliest Carboniferous (ca. 360–340 Ma; Dallmeyer et al. 1997) a massive allochthonous complex was progressively transported over the Iberian parautochthonous and autochthonous (Central Iberian Zone) domains (Figs. 1, 2; Díez Fernández and Arenas 2015; Díez Fernández et al. 2016 and references therein), which represent in NW Iberia the section of the Gondwanan margin that was not involved in subduction (Arenas et al. 2016). Coevally to the allochthonous units emplacement, the Iberian autochthon experienced shortening (D_1 folding and thrusting). The subsequent crustal evolution of NW Iberia was marked by a stage of gravitational collapse (D_2 folding and extensional shearing), and then followed by later subhorizontal shortening (D_3–D_4 folding and strike-slip shearing), defining the general structure of this part of the Variscan Orogen (Fig. 3; Díez Fernández and Pereira 2016 and references therein).

The compositional range of Carboniferous intrusions in the Iberian autochthonous domain represented by the Central Iberian Zone is wide. Most granitic rocks are S-type peraluminous, sometimes with abundant Al-rich minerals such as cordierite, sillimanite and andalusite. But there are also granitic rocks with transitional features between S- and I-type, I-type and hybrid granites, including rare metaluminous varieties (Bea et al. 1999, 2003; Castro et al. 1999, 2002; Fernández-Suárez et al. 2000, 2011; Neiva and Gomes 2001; Neiva et al. 2009; Dias et al. 1998, 2010; Teixeira et al. 2011; Villaseca et al. 2012; Merino Martínez et al. 2014). The type of sources for Variscan granites has been widely discussed. Crustal recycling of metasedimentary and metaigneous upper crustal sources, metasedimentary mid-crustal sources, metaigneous lower crustal sources, or mantle sources that interacted with distinct crustal melts is among the most cited (e.g., Neiva and Gomes 2001; Castro et al. 1999, 2002; Bea et al. 1999, 2003; Villaseca et al. 1999, 2012; Teixeira et al. 2011).

U–Pb zircon geochronology of the granitic rocks found in the Iberian autochthonous domain of the Central Iberian Zone indicates that part of the magmatic crystallization ages obtained overlap the time interval of development of Variscan structures (ca. 335–306 Ma; Dias et al. 1998; Bea et al. 1999; Villaseca and Herreros 2000; Castro et al. 1999, 2002; Valle Aguado et al. 2005; Teixeira et al. 2011; Díaz-Alvarado et al. 2011; Villaseca et al. 2012; Orejana et al. 2012; Martínez Catalán et al. 2014; Díez Fernández and Pereira 2016, 2017). The Permo-Carboniferous granitic rocks (ca. 306–287 Ma; Dias et al. 1998; Fernández-Suárez et al., 2011; Neiva et al. 2012; Villaseca et al. 2012; Orejana et al. 2012; Díez Fernández and Pereira 2017) crosscut Variscan structures and are considered as unrelated to the Gondwana-Laurussia collision sensu stricto (e.g., Gutiérrez-Alonso et al. 2011; Pereira et al. 2015a).

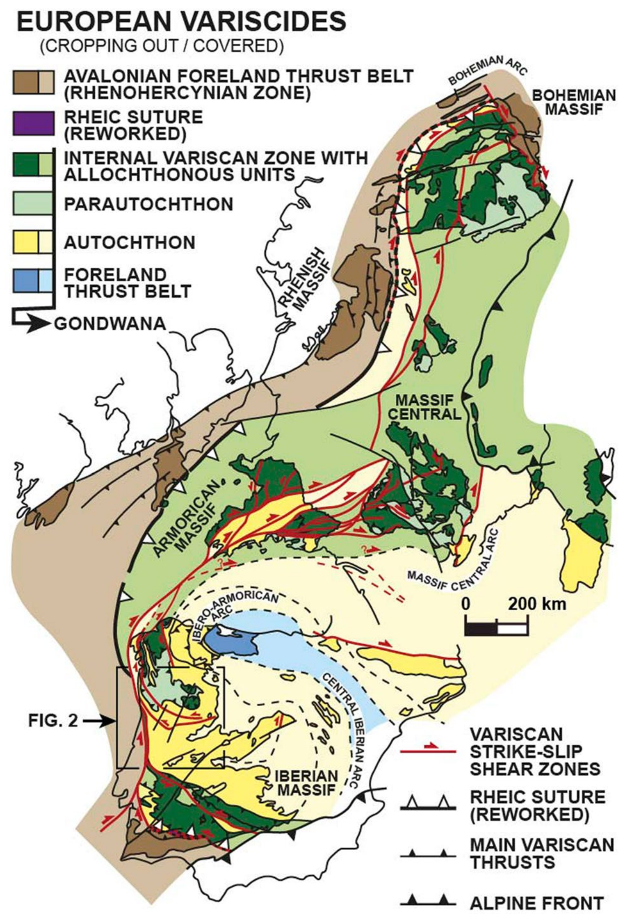

Fig. 1 Location of the study area in the Variscan orogen (adapted from Martínez Catalán et al. 2007 and Díez Fernández and Arenas 2015)

It has long been proven that the Variscan granitic rocks of the Central Iberia Zone have variable and complex spatial and temporal relationships between them (Julivert et al. 1974; Ugidos 1990) and with Variscan structures (Ferreira et al. 1987). However, the exact timing between the intrusions of some of the granite phases to the regional deformation–metamorphism is yet to be properly established. In this study, we report field data and U–Pb zircon geochronology of S-type granites from the Central Iberian Zone in Portugal (Mêda-Escalhão-Penedono Massif) to better: (i) constrain the timing of magma generation and emplacement (this is the first time that U–Pb zircon dating is applied to these plutons), (ii) analyze its relationship with a regional switch from D_2 extensional to D_3 contractional deformation, (iii) determine a possible source of the granitic magmas, and (iv) discuss the regional significance by comparing our results with equivalent data from the Variscan magmatism of SW Iberia. The field and geochronological data presented and discussed here contribute to a better understanding of models regarding pluton emplacement under different stages of collision orogenic deformation. This work is a tribute to the career of Prof. Jarda Dostal, who devoted much of his research to granites.

Geological setting

The stratigraphy of the Iberian autochthonous domain in the Central Iberian Zone is dominated by Neoproterozoic to Carboniferous siliciclastic sequences with minor volcanic and carbonate rocks (San José et al. 1990; Gutiérrez Marco et al. 1990; Rodríguez-Alonso et al. 2004; Martínez Poyatos et al. 2004) (Fig. 2).

Sequential Variscan deformation episodes are recognized by the overprinting relationships between different ductile structures, which may be more or less developed according to their heterogeneous spatial distribution and intensity. D_1 folds and thrusts (ca. 360–337 Ma; Dallmeyer et al. 1997; Escuder Viruete et al. 1998; Rubio Pascual et al. 2013; Díez Fernández et al. 2013; Dias da Silva et al. 2014) formed during early crustal thickening. Initial contractional deformation was followed by D_2 extensional deformation (Noronha et al. 1978; Escuder Viruete et al. 1994; Díez Balda et al. 1995; Rubio Pascual et al. 2013; Díez Fernández et al. 2013; Martínez Catalán et al. 2014; Díez Fernández and Pereira 2016) responsible for the exhumation of high-grade rocks (ca. 337–316 Ma; Escuder Viruete et al. 1994, 1998; Barbero 1995; Dallmeyer et al. 1997; Castiñeiras et al. 2008; Martínez Catalán et al. 2014; Díez Fernández and Pereira 2016). D_3 upright folds are widespread in the region and show consistent trend and axial planar foliation (S_3), but are locally affected by Variscan D_{3-4-5} strike-slip shear zones (Díez Fernández and Pereira 2016, 2017) (Fig. 3).

Voluminous Variscan magmatic activity in the Central Iberian Zone has been usually interpreted to be restricted to the time interval in which D_3 contractional deformation was active, from ca. 321 Ma to ca. 300 Ma, following the classification of Ferreira et al. (1987). This assumption is not fully supported by field and U–Pb zircon data, which suggest a spatial and temporal relationship between voluminous magmatism and the transition from the waning stages of D_2 extensional deformation to the early stages of D_3 contraction (Díez Fernández and Pereira 2016).

Variscan basement (Moimenta da Beira-Pinhel region)

Stratigraphy, deformation and metamorphism

In the Portuguese sector of the Central Iberian Zone (Moimenta da Beira-Pinhel region), the lithostratigraphy is variably metamorphosed and comprises (Regêncio Macedo 1988; Sousa and Sequeira 1989; Silva and Ribeiro 1991, 1994; Oliveira 1992; Ferreira and Sousa 1994): Cambrian greywackes, siltstones, pelites and limestones (Schist-Greywacke Complex: Douro Group) unconformably overlain by Ordovician felsic volcaniclastic rocks (São Gabriel Formation), which are subsequently overlain by sandstones, siltstones and mudstones (Armorican Quartzite Formation) (Fig. 4).

The pelites, sandstones, greywackes and volcanic rocks were transformed into slate, quartzite, phyllite, schist, gneiss and migmatite as a result of variable metamorphic conditions attained during Variscan deformation. Variations in metamorphic grade are sharp along a formerly low-dipping D_2 extensional shear zone (i.e., Pinhel shear zone), whose hanging wall and footwall define at a regional scale a low- (LGD) and a high-grade (HGD) domain, respectively (Díez Fernández and Pereira 2016). The Pinhel shear zone was folded during D_3 contraction, and then deformed by D_{3-4-5} strike-slip shear zones under lower grade metamorphic conditions (Huebra, Lamego-Malpica, Juzbado-Penalva do Castelo and Porto-Tomar shear zones; Díez Fernández and Pereira 2016, 2017) (Fig. 4).

Magmatism

In the Moimenta da Beira-Pinhel region, the Variscan intrusions classify in three age groups from Serpukhovian to Moscovian, including strongly and variably deformed granitic rocks: syn-D_2 (ca. 331–321 Ma), late D_2-early D_3 (ca. 317–315 Ma) and syn-D_3 (ca. 311–310 Ma) (Díez Fernández and Pereira 2016).

The syn-D_2 granitic rocks are spatially and temporally related to migmatites of the HGD (Fig. 4). They are fine- to coarse-grained (sometimes resembling diatexite migmatites), and their facies range from poorly deformed to strongly foliated two-mica granites, with S_2 foliation defined by mica oriented parallel to the elongate shape of quartz (including subgrains and newly formed grains) and feldspar. These granites intruded at ca. 331–321 Ma, based on zircon U–Pb ages (Díez Fernández and Pereira 2016).

The late D_2-early D_3 Ucanha-Vilar Massif is a 25 km long, NW–SE elongated body made of porphyritic medium–coarse-grained biotite-rich granitic rocks including granodioritic–tonalitic enclaves (Fig. 4). These granodiorites and monzogranites are characterized by a dominant steeply dipping planar anisotropy defined by the alignment of feldspar phenocrysts, and preferred orientation of biotite and microgranular mafic enclaves. The NW–SE to N–S-striking magmatic foliation is locally folded and deformed by discrete N70E-striking D_4 strike-slip shear zones. This pluton intruded at ca. 317–315 Ma, based on zircon and monazite U–Pb ages (Dias et al. 1998; Simões 2000).

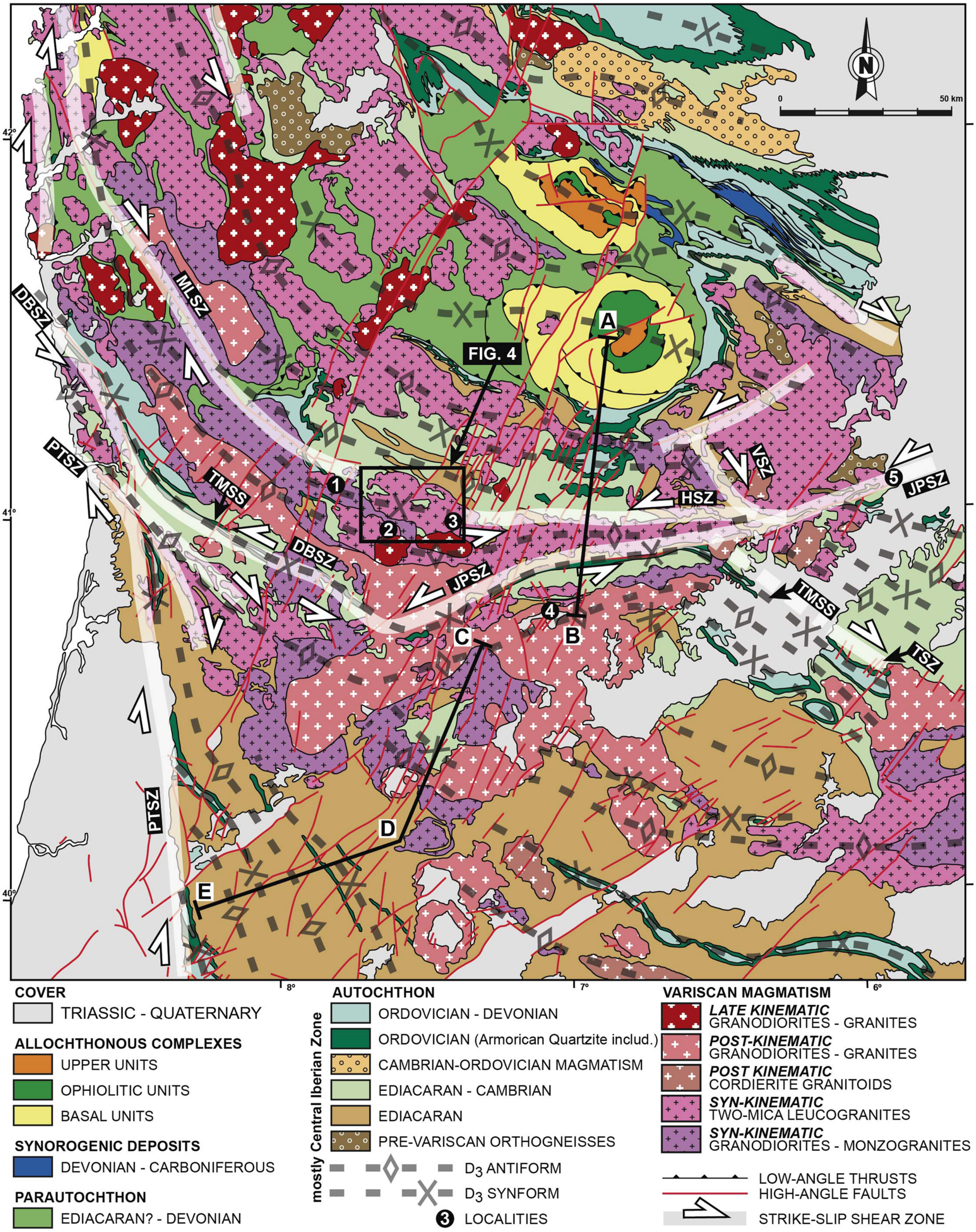
N
0
50 km
42°
41°
40°
8°
7°
6°
DBSZ
MLSZ
PTSZ
TMSS
JPSZ
HSZ
VSZ
TSZ
FIG. 4
A
B
C
D
E
1
2
3
4
5
COVER
TRIASSIC - QUATERNARY
ALLOCHTHONOUS COMPLEXES
UPPER UNITS
OPHIOLITIC UNITS
BASAL UNITS
SYNOROGENIC DEPOSITS
DEVONIAN - CARBONIFEROUS
PARAUTOCHTHON
EDIACARAN? - DEVONIAN
AUTOCHTHON
mostly Central Iberian Zone
ORDOVICIAN - DEVONIAN
ORDOVICIAN (Armorican Quartzite includ.)
CAMBRIAN-ORDOVICIAN MAGMATISM
EDIACARAN - CAMBRIAN
EDIACARAN
PRE-VARISCAN ORTHOGNEISSES
D3 ANTIFORM
D3 SYNFORM
LOCALITIES
VARISCAN MAGMATISM
LATE KINEMATIC GRANODIORITES - GRANITES
POST-KINEMATIC GRANODIORITES - GRANITES
POST KINEMATIC CORDIERITE GRANITOIDS
SYN-KINEMATIC TWO-MICA LEUCOGRANITES
SYN-KINEMATIC GRANODIORITES - MONZOGRANITES
LOW-ANGLE THRUSTS
HIGH-ANGLE FAULTS
STRIKE-SLIP SHEAR ZONE

◂**Fig. 2** Regional map of the central part of the Iberian Massif (after Díez Fernández and Pereira 2016). The trace of mayor faults, late upright folds, and strike-slip shear zones is shown. Localities (numbered black circles): *1* Lamego; *2* Moimenta da Beira; *3* Penedono; *4* Pinhel; *5* Juzbado. *DBSZ* Douro-Beira shear zone, *HSZ* Huebra shear zone, *JPSZ* Juzbado-Penalva do Castelo shear zone, *MLSZ* Malpica-Lamego shear zone, *PTSZ* Porto-Tomar shear zone, *TMSS* Tamames-Marofa-Sátão Synform, *TSZ* Tamames shear zone, *VSZ* Villalcampo shear zone. Geographic coordinates

Previous field studies (Ferreira and Sousa 1994) suggested a coeval nature of these granitoids with the two-mica granites of the Mêda-Escalhão-Penedono pluton and some hecto–decameter-scale bodies of granodiorite/quartzdiorite. Both massifs occur at the core of D_3 upright antiforms (Fig. 4).

The syn-D_3 Tabuaço Massif is a NW–SE elongated, oval shaped body (8 km wide and 35 km long) of granitic rocks that intrude the Pinhel shear zone and the late D_2-early D_3 Mêda-Escalhão-Penedono Massif (Fig. 4). The Tabuaço pluton is made of fine- to coarse-grained, muscovite-rich (rarely porphyritic) and two-mica (partially porphyritic) granites dated at ca. 310 Ma, based on zircon U–Pb ages (Neiva et al. under review). It includes xenoliths and roof pendants of the HGD. This massif shows near-vertical planar anisotropy and kinematic criteria that suggest it was affected by the sinistral strike-slip shearing that concentrated along the D_3 Huebra and D_4 Juzbado-Penalva do Castelo shear zones. Towards southwest, in the Pinhel region, the Santa Eufémia Massif represents an E–W elongated, oval shaped body of medium-grained two-mica syn-D_3 granite. It shows preferred orientation of quartz (undulose extinction and subgrains), feldspar and micas defining a moderate S_3 subvertical planar anisotropy. It cuts the LGD-HGD boundary of the D_2 Pinhel shear zone and occurs at the core of a D_3 antiform. The crystallization age of that D_3 granite was estimated at ca. 311 Ma, based on zircon U–Pb ages (Díez Fernández and Pereira 2016).

Mêda-Escalhão-Penedono Massif

The Mêda-Escalhão-Penedono Massif is a 10–15 km wide and 80 km long body of coarse- to medium-grained two-mica granites elongated in the ENE–WSW to ESE–WNW directions (Figs. 2, 4). It shows a magmatic fabric defined by the preferred orientation of mica, micaceous enclaves (Fig. 5a, b) and schlieren layering (Fig. 6c). The magmatic fabric is transposed by S_3 cleavage (Fig. 5c, d). This massif includes xenoliths of the HGD rocks and cuts the LGD-HGD boundary. The generally diffuse nature of the contacts between two-mica granite and S_2 compositional layering/foliation of the HGD host rocks evidence they are rather contemporaneous (Fig. 5c, d). D_3 contraction was responsible for folding the S_2 compositional layering/foliation of the host metamorphic rocks (Fig. 5c, d). The Mêda-Escalhão-Penedono pluton has interfingering contacts with the late D_2-early D_3 Ucanha-Vilar Massif suggesting they are coeval intrusions. Discordant and mutually crosscutting contact between the two-mica granite dykes and the biotite-rich porphyritic monzogranite indicate that they were emplaced at the same time interval (Figs. 5e, 6a, d).

Along the northern contact of the Mêda-Escalhão-Penedono Massif two sets of pervasive S-C mylonitic fabrics are recognized. Subvertical mylonitic bands striking N80E (sinistral) and N120E (dextral) are the result of strike-slip motions associated with the D_3 Huebra and Malpica-Lamego shear zones, respectively. These regional shear zones and the local mylonitic bands run roughly parallel to the axial planes of D_3 folds. The Mêda-Escalhão-Penedono Massif is also affected by later, N70E-striking (sinistral), discrete strike-slip shear zones, which are probably subsidiary to the D_4 Juzbado-Penalva do Castelo shear zone (Fig. 6b).

The Mêda-Escalhão-Penedono S-type calc-alkaline peraluminous granites ($SiO_2 = 71.1$–73.7 wt%; $Al_2O_3 = 14.2$–15.3 wt%, $MgO = 0.3$–0.4 wt%, $Fe_2O_3 = 0.1$–0.5 wt%, $TiO_2 = 0.1$–0.3 wt%, $CaO = 0.6$–0.9 wt%, $Na_2O = 3.4$–4.6 wt%, $K_2O = 5.0$–5.1 wt%) include two main varieties (e.g., Ferreira and Sousa 1994) that were sampled for geochronology. Sample MB-1 is a fine- to medium-grained biotite (dominant)–muscovite granite (partially porphyritic) consisting of quartz, perthitic K-feldspar and plagioclase (albite and albite–oligoclase). Sillimanite, apatite, zircon, monazite, tourmaline, chlorite and ilmenite are accessory minerals. Samples MB-2 and MB-3 are medium- to coarse-grained muscovite (dominant)–biotite granites (partially porphyritic) consisting of quartz, perthitic K-feldspar and plagioclase (albite). Apatite, tourmaline, sericite, zircon, chlorite and ilmenite are accessory minerals. These granites display highly evolved isotopic signatures of $\varepsilon_{Nd} < -7$ (Dias et al. 2002).

Along the intrusive contact with the host HGD rocks, the late D_2-early D_3 two-mica granites typically occur as conformable and discontinuous 1–20 m thick dykes resembling diatexite migmatite (Fig. 6c). Some granite dykes intruded parallel to the compositional layering of the host high-grade metamorphic rocks, being folded and boudinaged during D_2 deformation (Fig. 6d).

Zircon U–Pb geochronology

Analytical method

Zircon grains were obtained from three samples of granite with standard heavy mineral separation techniques. They

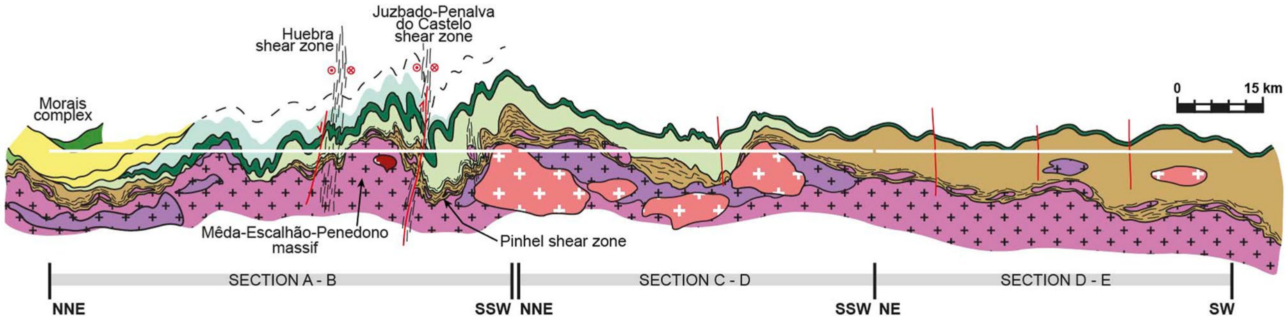

Fig. 3 Synthetic composite geological section across the southern part of the Central Iberian Zone (after Díez Fernández and Pereira 2016). The cross section is normal to D_2 (orogen-parallel) tectonic flow, but is intended to best show the D_3 upright fold structure of the region. The direction of emplacement of the allochthonous complexes (e.g., Morais Complex) (D_1) is to the E–SE (Ribeiro et al. 1990; Martínez Catalán et al. 2009). The legend and trace of the composite cross section is indicated in Fig. 2

were mounted in epoxy resin, polished down to equatorial sections and photographed at University of Évora. Zircon was imaged by SEM cathodoluminescence at TU Bergakademie, Freiberg and analyzed for U, Th, and Pb isotopes by LA-ICP-MS at the Museum für Mineralogie und Geologie (Senckenberg Naturhistorische Sammlungen Dresden), using a Thermo-Scientific Element 2 XR sector field ICP-MS coupled to a New Wave UP-193 Excimer Laser System. To enable sequential sampling of heterogeneous grains (e.g., growth zones) during time resolved data acquisition a teardrop-shaped, low volume laser cell was used. Each analysis (laser spot-sizes of 15–35 µm) consisted of 15 s background acquisition followed by 35 s sample acquisition. A common Pb correction based on the interference- and background-corrected ^{204}Pb signal and a model Pb composition (Stacey and Kramers 1975) was applied if necessary. The necessity of the correction was judged on whether the corrected ^{207}Pb/^{206}Pb lies outside of the internal errors of the measured ratios. An in-house Excel® spreadsheet program developed by Dr. Axel Gerdes (Institute of Geosciences, Johann Wolfgang Goethe-University Frankfurt, Frankfurt am Main) was used to correct raw data for background signal, common Pb, laser-induced elemental fractionation, instrumental mass discrimination, and time-dependent elemental fractionation of Pb/Th and Pb/U. Reported uncertainties were propagated by quadratic addition of the external reproducibility obtained from the standard zircon GJ-1 during individual analytical sessions (~0.6 and 0.5–1% for the ^{207}Pb/^{206}Pb and ^{206}Pb/^{238}U, respectively), and from the within-run precision of each analysis. Plotting of U–Pb data was performed using Isoplot (Ludwig 2001). In this study, the ^{207}Pb/^{206}Pb ages were taken for interpretation for all zircon >1.0 Ga, and the ^{206}Pb/^{238}U ages for younger grains (for details see Frei and Gerdes 2009). Pb-loss was inferred for few strongly discordant analyses and for some anomalously young concordant U–Pb ages.

Results

The U–Pb results of magmatic and inherited zircon are given in Table 1 (supplementary data repository). Concordia and probability density diagrams are presented together with CL imaging of representative zircon grains (Fig. 7). The three samples of S-type two-mica granites (Fig. 4 for sample location) contain zircon grains (60–310 µm diameter) with common features. They have a wide range of morphologies, from rounded subhedral to prismatic euhedral. Prisms are equant to moderately elongate (aspect ratios 1:4). The internal structure of most grains is quite complex, including cores with simple concentric zoning, banded zoning, one or more overgrowths and even unzoned sectors. A concentric zoned or unzoned rim surrounds most cores (Fig. 7).

Sixty-four analyses were obtained from 60 zircon grains from sample MB-1 (Supplementary Table 1). Of a total of 33 concordant analyses (90–110% concordance; Fig. 7a), 54.5% represents Carboniferous grains. The best estimate for the crystallization age of the granite is a Concordia age of 317 ± 3 Ma (MSWD = 0.15) (Fig. 7b). This age was obtained after rejecting the youngest Carboniferous age (ca. 299 Ma) and a “Permian” age (ca. 293 Ma), which together probably reflect later recrystallizations. The older zircon grains are interpreted to be inherited grains: Ediacaran and Cryogenian (ca. 659–552 Ma; 33.3%), Cambrian (ca. 537 Ma; 3%), Ordovician (ca. 473 Ma; 3%) and Paleoproterozoic (ca. 2 Ga; 3%).

We performed 59 analyses in 58 zircon grains from sample MB-2 (Supplementary Table 1).

Of a total of 33 concordant analyses (90–110% concordance; Fig. 7a), 21.2% represents Carboniferous grains. The best estimate for the crystallization age of the granite is a Concordia age of 319 ± 4 Ma (MSWD = 0.002) (Fig. 7c). The youngest ages (“Permian”) probably reflect a later hydrothermal recrystallization. The most abundant

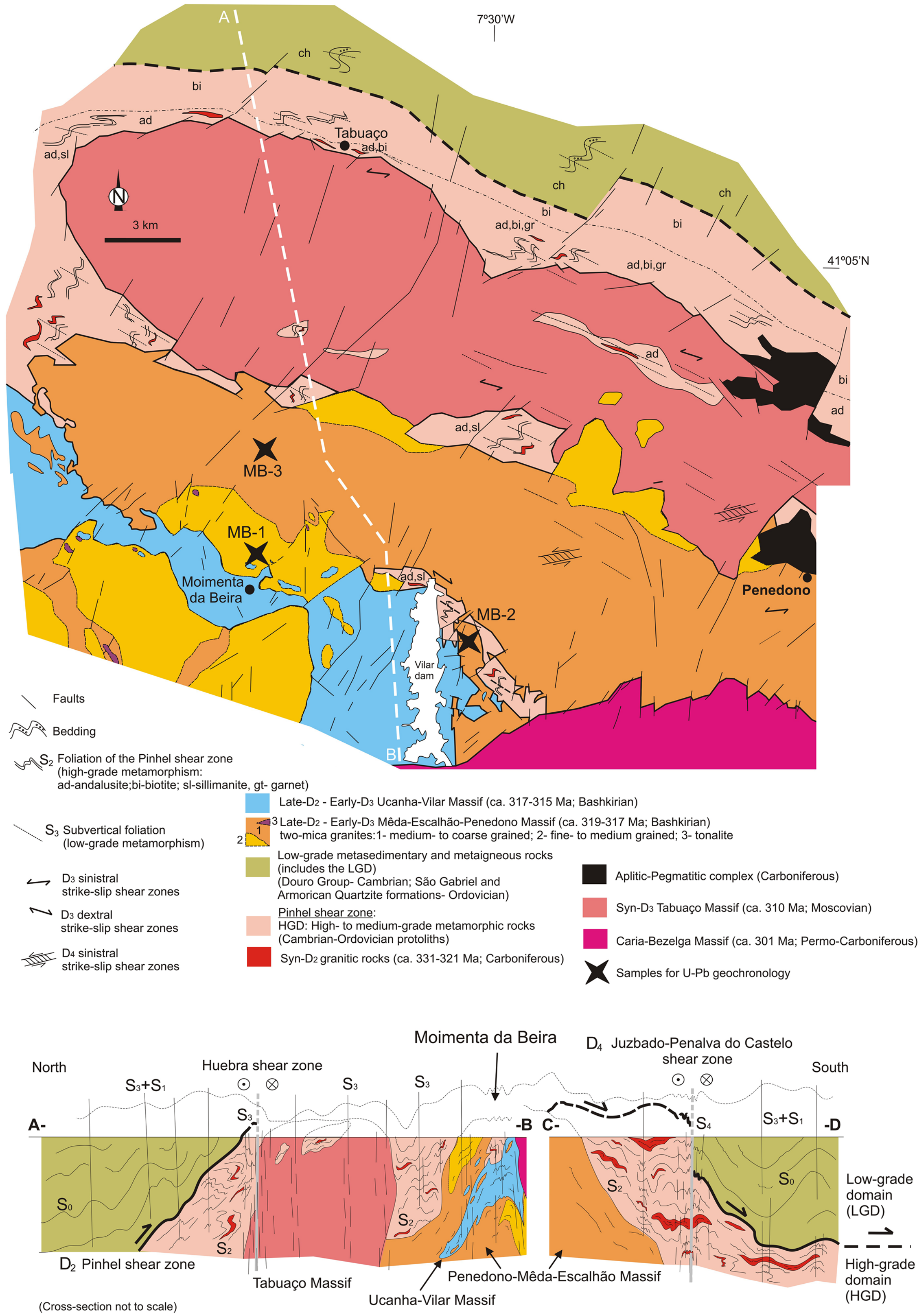

Fig. 4 Schematic geological map of Moimenta da Beira region after Sousa and Sequeira (1989), Oliveira (1992) and Ferreira and Sousa (1994). Sampling locations of Bashkirian S-type granites are indicated with *black stars*. The composite cross section includes *A–B* (data from this work) and *C–D* (following Díez Fernández and Pereira 2016)

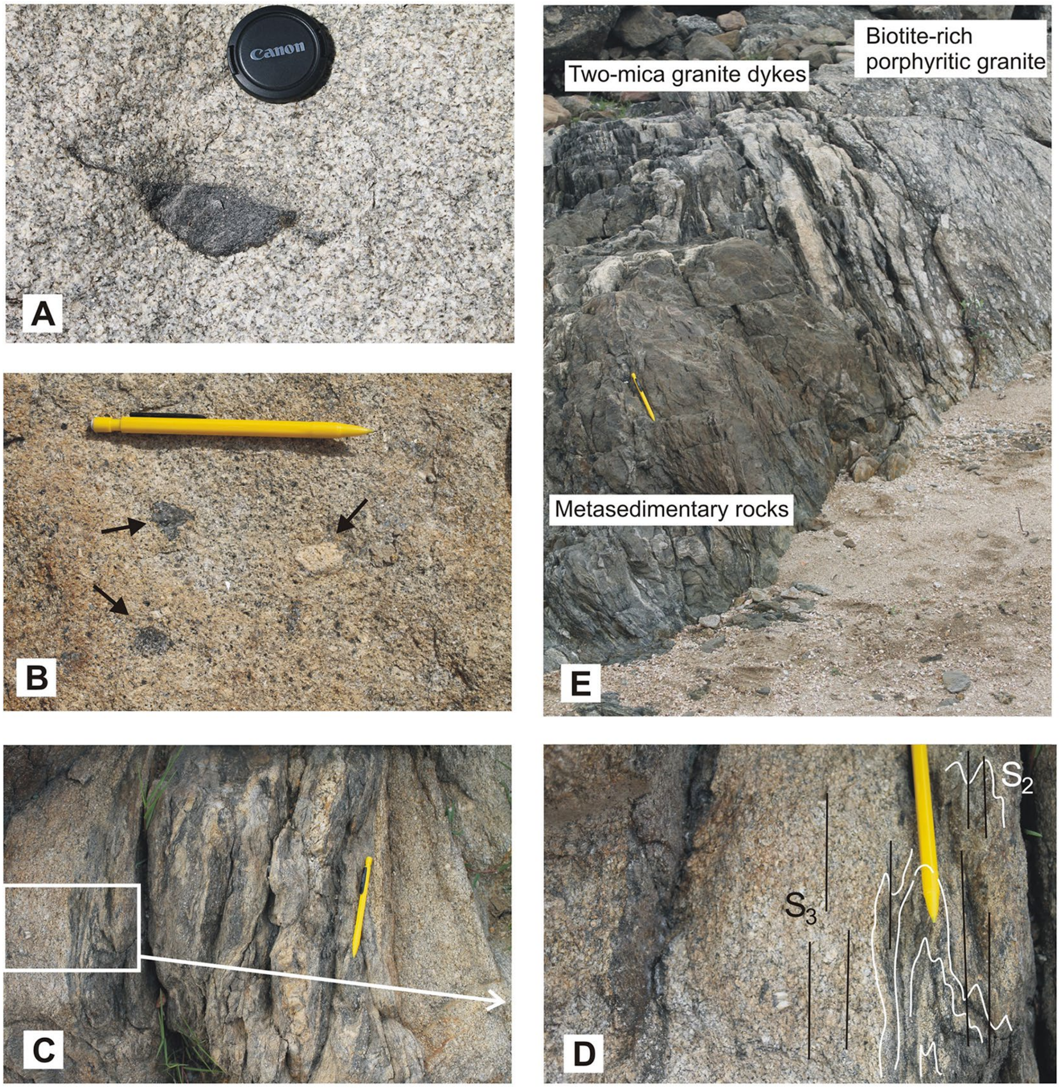

Fig. 5 Late D_2-early D_3 two-mica granite of the Mêda-Escalhão-Penedono Massif with **a**, **b** micaceous enclaves and **b** feldspar phenocrysts; **c**, **d** diffuse nature of the contacts between two-mica granite and S_2 compositional layering/foliation of the HGD host metasedimentary rocks, transposed by S_3. **e** Two-mica granite dykes cutting the HGD metasedimentary rocks (*left*) and discordant and mutually crosscutting contact between the two-mica granite dykes and the biotite-rich porphyritic monzogranite (*right*)

inherited grains are Ediacaran and Cryogenian (ranging from ca. 816 to ca. 558 Ma; 45.5%), followed by Paleoproterozoic (ca. 1.9 Ga; 9.1%), Cambrian (ca. 516–514 Ma; 6.1%), Ordovician (ca. 460–466 Ma; 6.1%) and Silurian (ca. 433–421 Ma; 6.1%).

Sixty-one analyses were carried out in 61 zircon grains from sample MB-3 (Supplementary Table 1). Of a total of 33 concordant analyses (90–110% concordance; Fig. 7a), 27.3% accounts for Carboniferous grains. The best estimate for the crystallization age of the granite is a Concordia age of 319 ± 2.6 Ma (MSWD = 1.5) (Fig. 7d). The most abundant group of inherited grains is Ediacaran and Cryogenian (ranging from ca. 696 to ca. 549 Ma; 36.4%); other inherited grains gave Cambrian (ca. 511–500 Ma; 12.1%), Paleoproterozoic (ca. 1.9 Ga; 9.1%), Ordovician (ca. 468–456 Ma; 6.1%), Mesoproterozoic (ca. 1 Ga; 6.1%) and Neoarchean (ca. 2.57 Ga; 3%) ages.

Discussion

Age of magmatic zircon grains and rims

The emplacement age of the two-mica granites of the Mêda-Escalhão-Penedono Massif is estimated at 318.7 ± 4.8 Ma (weighted average age obtained from 33 analyses—34.7%; MSWD = 0.22, probability = 1) based

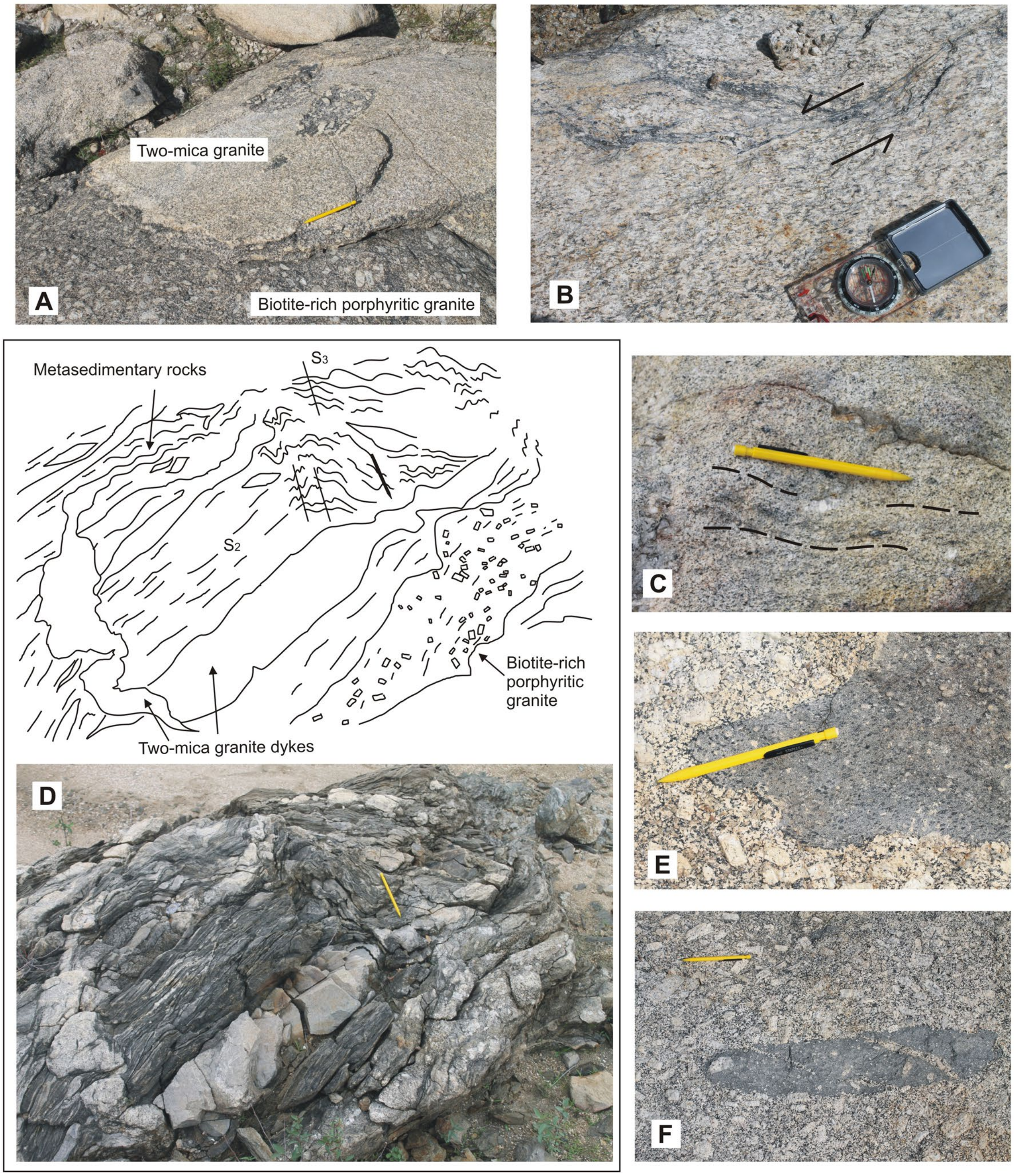

Fig. 6 **a** Discordant and mutually crosscutting contact between the two-mica granite dykes and the biotite-rich porphyritic monzogranite; **b** N70E-striking (sinistral), discrete D_4 strike-slip shear zones affecting the late D_2-early D_3 two-mica granite; **c** two-mica granite with schlieren layering resembling diatexite migmatite; **d** discordant, conformable and discontinuous two-mica granite and biotite-rich porphyritic monzogranite dykes cutting the HGD host metamorphic rocks; granitic dykes are folded and boudinaged by D_2; **e**, **f** mafic microgranular enclaves (granodioritic–tonalitic) included in the porphyritic monzogranite

on euhedral grains and concentric zoned rims found on almost all zircon grains (Fig. 8a, b).

The Mêda-Escalhão-Penedono two-mica granites have the same age as the granitic rocks of the biotite-rich granodiorites and monzogranites from the Lamego and Ucanha-Vilar massifs (ca. 319–317 Ma; Simões 2000; Dias et al. 2002). This result was expected because the two massifs exhibit interfingering contacts indicating they are coeval. A relevant finding is that the emplacement age of these granitic rocks overlaps the time interval for the maximum tectonomagmatic activity of the Pinhel shear zone (ca. 321–317 Ma; Díez Fernández and Pereira 2016), supporting the

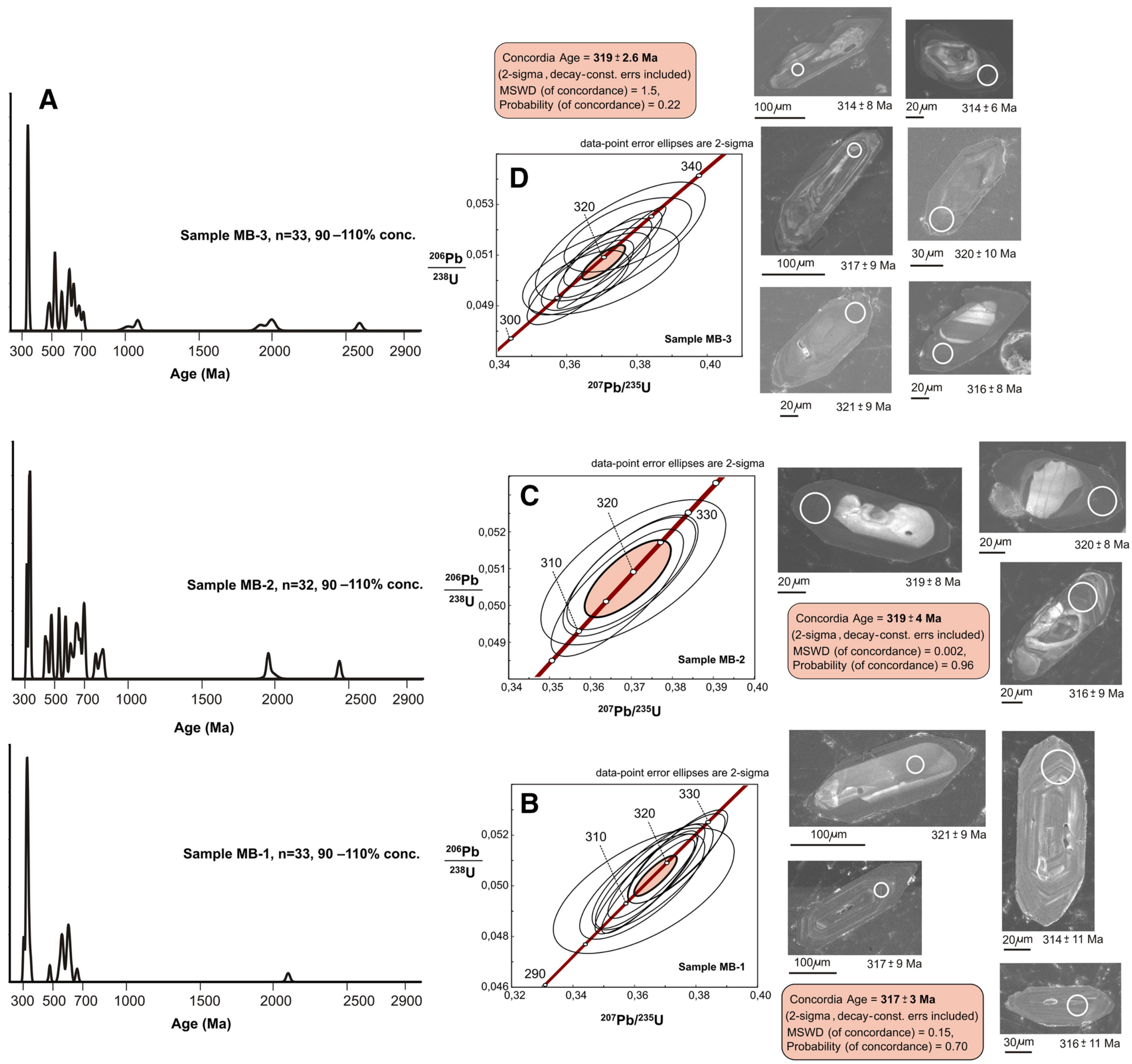

Fig. 7 **a** Probability density plot of U–Pb zircon ages from S-type granites of the Moimenta da Beira region; **b–d** Concordia plots with the youngest U–Pb zircon ages (Carboniferous) for all three analyzed samples (90–110% concordance), samples MB-1, MB-2 and MB-3 respectively. Cathodoluminescence (CL) images with reference to analyzed spots of Carboniferous zircon grains

correlation between magma generation and D_2 extensional deformation reaching high-grade metamorphic conditions of anatexis. The HGD rocks of the D_2 Pinhel shear zone show evidence of partial melting and close spatial relationship with different generations of granitic dykes (resembling diatexite migmatites) intruded subparallel or discordant to the S_2 foliation and compositional layering.

Metamorphic mineral assemblages of the HGD rocks indicate temperature and pressure conditions during metamorphism of 725 ± 50 °C and 5.4 ± 1 kbar, implying relatively shallow depths (at least 15 km) for crustal anatexis (Pereira et al. 2014). This suggests that the metamorphic recrystallization and partial melting in the Pinhel shear zone, and the magma production and emplacement of the Mêda-Escalhão-Penedono and Ucanha-Vilar plutons were part of the same thermal event.

Age of inherited zircon: implications for S-type magma genesis

The oldest inherited zircon grains in the Mêda-Escalhão-Penedono granitic rocks are Palaeoproterozoic (ca.

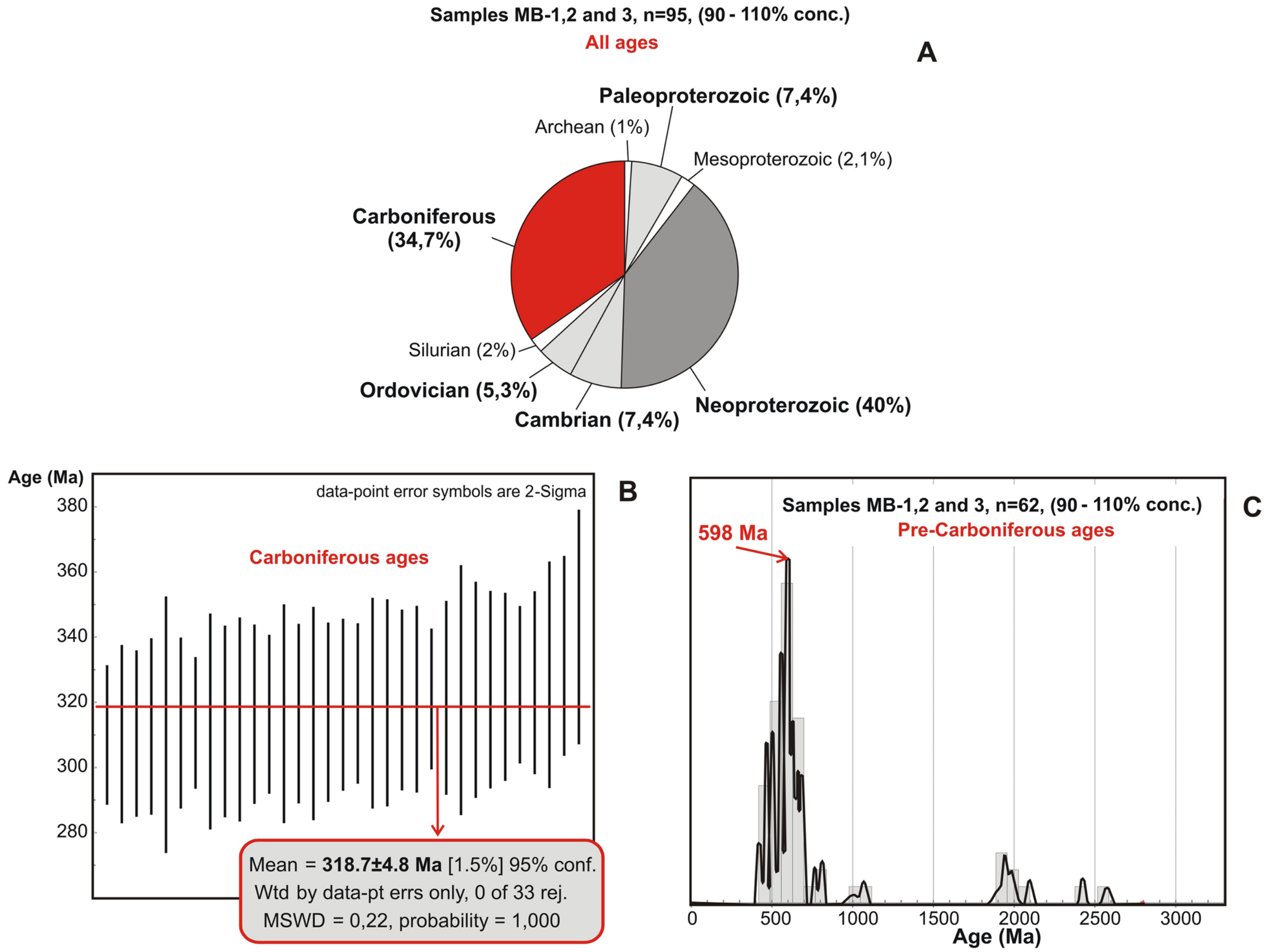

Fig. 8 **a** Pie diagram with U–Pb zircon ages for all three analyzed samples (90–110% concordance); **b** weighted average age of the youngest U–Pb zircon ages (Carboniferous) for all three analyzed samples (90–110% concordance); *MSWD* mean square of weighted deviates; **c** Age histogram and Probability density plot including the oldest U–Pb zircon ages (pre-Carboniferous)

2.4–1.9 Ga; 7.4%), Mesoproterozoic (ca. 1 Ga; 2.1%), and Neoarchean (ca. 2.57 Ga; 1%) (Fig. 8a, c). The Ediacaran and Cryogenian age group is the largest one (40%) and peaks at ca. 598 Ma (Fig. 8c), thus matching the ages of Pan-African and Cadomian zircon forming events (e.g., Pereira 2015 and references therein). The Precambrian inherited zircon ages closely resemble the age spectrum of detrital zircon from the Ediacaran (Beiras Group; Pereira et al. 2012a; Talavera et al. 2012) and Cambrian (Douro Group; Teixeira et al. 2011; Talavera et al. 2012) metasedimentary rocks of the Iberian autochthonous domain.

Twelve inherited cores gave Cambrian and Ordovician ages that mostly overlap the time interval of some pre-Variscan magmatic events in the Iberian autochthon (ca. 498–462 Ma; Valverde-Vaquero and Dunning 2000; Talavera et al. 2013) and parauthochton (ca. 499–462 Ma; Talavera et al. 2013; Farias et al. 2014; Dias da Silva et al. 2014, 2016).

The youngest inherited cores found in the Carboniferous S-type granites give Silurian ages (ca. 433–421 Ma; 2%). Assuming that these ages have not been reduced by radiogenic Pb-loss, they place an upper limit of Silurian on the age of the crustal component of the granite magma. Such Silurian ages are coincident, within analytical error, with the zircon U–Pb age obtained for felsic volcanic rocks of the Iberian parautochthonous (439.6 ± 5 Ma; Valverde-Vaquero et al. 2007) and autochthonous (González Clavijo and Martínez Catalán 2002) domains.

U–Pb age determinations on inherited zircon extracted from the Mêda-Escalhão-Penedono granites are similar to those of their metamorphic host, indicating they probably formed by partial melting of Ediacaran to Silurian sedimentary and igneous rocks of the Iberian autochthonous domain. A similar crustal source was also proposed for the S-type peraluminous granites with similar age (ca. 317–316 Ma), geochemical (SiO_2 = 68.2–74.1

wt%; Al_2O_3 = 14.1–16.0 wt%, MgO = 0.2–0.9 wt%, Fe_2O_3 = 0.3–0.9 wt%, TiO_2 = 0.1–0.6 wt%, CaO = 0.5–0.9 wt%, Na_2O = 2.9–4.1 wt%, K_2O = 4.3–5.7 wt%) and isotopic composition ($\mathcal{E}_{Nd}$ = −9 to −8) of the Carrazeda de Ansiães Massif (Teixeira et al. 2007; Teixeira 2008). The existence of several S-type granite plutons of the same age (ca. 319–317 Ma), and derived from a crustal source that records protracted recycling of an older crust, demonstrates unequivocally that there was a major crustal recycling event in the Iberian autochthonous throughout Bashkirian times.

Field relationships and U–Pb data show that the Mêda-Escalhão-Penedono two-mica granites are spatially and temporally associated with the Ucanha-Vilar biotite-rich porphyritic granitic rocks. Therefore, Bashkirian crustal recycling via partial melting and anatexis gave rise to distinct magmas. The porphyritic granites are moderately peraluminous (SiO_2 = 62.1–68.9 wt%; Al_2O_3 = 15.2–16.4 wt%, MgO = 0.2–2 wt%, Fe_2O_3 = 2.8–5 wt%, TiO_2 = 0.4–0.6 wt%, CaO = 1.7–3.3 wt%, Na_2O = 3–3.3 wt%, K_2O = 4.8–5.1 wt%) and less enriched ($\mathcal{E}_{Nd}$ = −4.4 to −4.8) than the two-mica granites (e.g. Simões 2000; Dias et al. 2002). The first ones include mafic microgranular enclaves (granodioritic–tonalitic; Fig. 6e, f) that may account for magma mixing. Partial melting of a compositionally heterogeneous crust made of immature metasedimentary and/or felsic metaigneous rocks was proposed as their likely source (Dias et al. 1998, 2002). Another evidence for the coexistence of magmas with different composition is given by hecto- to decameter-scale bodies of foliated, fine-grained granodiorites/quartzdiorites that occur within the two-mica granites (Ferreira and Sousa 1994). These enclaves are slightly metaluminous (SiO_2 = 57.9 wt%; Al_2O_3 = 17.3 wt%, MgO = 2.6 wt%, Fe_2O_3 = 6.3 wt%, TiO_2 = 1.0 wt%, CaO = 4.1 wt%, Na_2O = 3.9 wt%, K_2O = 3.7 wt%), and have relatively unevolved isotopic compositions ($\mathcal{E}_{Nd}$ = −3.3) when compared to the two-mica granites and the porphyritic granitic rocks, suggesting an hybrid source (Simões 2000; Dias et al. 2002). The coeval input of mafic magma into the crust is another reasonable hypothesis for explaining the source of hybrid magmas (e.g., Castro et al. 1999) that was proposed as the driving mechanism for S-type melt production (e.g., Valle Aguado et al. 2005). However, the generation of the Bashkirian S-type granites at shallow crustal levels seems to have been dominated by continental crust recycling, rather than by addition of new material from the mantle.

Model of S-type granite emplacement

The ca. 319–317 Ma S-type granites make up a great extent of the surface geology in the Iberian autochthonous domain. Crustal melting at this scale probably required a combination of hot mid-crust and mantle-derived heat input at the base of the continental crust to produce extensive melting zones. The Mêda-Escalhão-Penedono S-type granite magmas are largely sourced from an Ediacaran-Cambrian greywacke–pelite sequence and, possibly, from Cambrian-Ordovician volcano-sedimentary sequences of the Iberian autochthonous domain. Although we have only found two Silurian grains (with a limited statistical significance) we cannot exclude the hypothesis that Silurian rocks from autochthonous domain were also a source of these granites. Inherited zircon cores from S-type granites of Carrazeda de Ansiães Massif match the age spectra shown by detrital zircon grains of metasedimentary rocks from the Cambrian Beiras Group, mainly in the Ediacaran-Cryogenian time interval (Teixeira 2008; Teixeira et al. 2011). The tectonothermal record of the study area is similar to that presented by Díez Fernández and Pereira (2016) for a region located nearby to the east. Consequently, an equivalent (adapted) evolutionary model may be applied to explain the sequence of Variscan events recorded in the study area. Underthrusting and crustal thickening (D_1 contractional deformation) are considered responsible for creating a thermally and gravitationally imbalanced crust during the early stages of Gondwana-Laurussia collision (Escuder Viruete et al. 1994; Martínez Catalán et al. 2014; Alcock et al. 2015) (Fig. 9a). The resulting gravitational disequilibrium was progressively attenuated by pervasive extensional flow that operated on overthickened sections of the Variscan orogen (e.g., Pinhel shear zone; D_2 extensional deformation), thus facilitating heat advection from lower parts of the crust and the mantle along with a progressive thermal recovery after a period of thermal maturation. D_2 extensional deformation favored partial melting and anatexis of fertile layers within the crust. Thermal and gravitational reequilibration were assisted by large-scale mass and heat transfer upwards through the crust, as indicated by the generation and emplacement of S-type granitic magmas into the upper crust at ca. 331–317 Ma (Fig. 9b). Magma genesis peaked at ca. 321–317 Ma, as indicated by the age of large late-D_2 intrusions cutting across the Pinhel shear zone (Díez Fernández and Pereira 2016; data in this work).D_2 extension has been framed in an intra-orogenic setting, i.e. Gondwana and Laurussia continued to move relative to each other during Variscan extensional collapse (Martínez Catalán et al. 2007; Díez Fernández et al. 2012, 2016). A progressive decrease of the post-D_1 gravitational disequilibrium in this context led to a regional switch from widespread subhorizontal extension to compression, probably derived from further convergence between Gondwana and Laurussia. Renewed compression brought in the cessation of D_2 extensional shear zones along with the onset and amplification of D_3 upright folds and strike-slip shear zones (Fig. 9c). S-type magmatism did not decline immediately

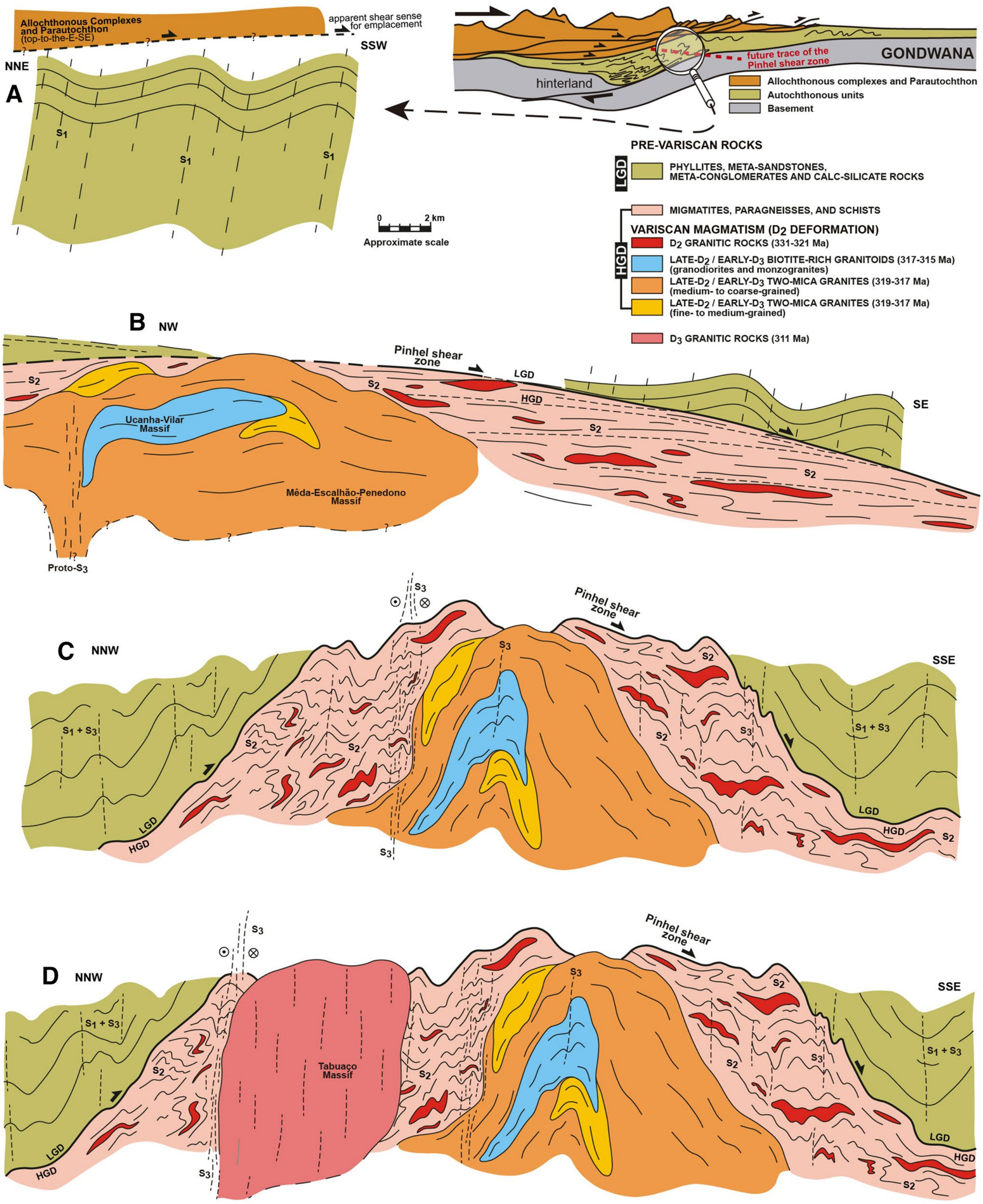

Fig. 9 Idealized model showing the tectonometamorphic evolution (D_1–D_3) of the study area (following Díez Fernández and Pereira 2016). See text for explanation. Location of the Pinhel shear zone in a simplified orogenic model is shown in the *upper right part*

after crustal extension, as it remained during D_3 (Fig. 9d). The simultaneous emplacement of granitic rocks with variable geochemical and isotopic compositions, from highly ($\mathcal{E}_{Nd} < -7$) to relatively unevolved isotopic compositions ($\mathcal{E}_{Nd} = -3.3$), suggest that high-grade metamorphic conditions were reached in a compositionally heterogeneous crust (e.g., Dias et al. 2002) after the time required for thermal recovery. Part of such heterogeneity was transferred from the source to the upper crust via partial melting and melts migration, as reflected by crustal-derived granitic massifs emplaced during crust attenuation. Syn-orogenic extensional collapse assisted this process, and is regarded here as a mechanism capable of probing unexposed levels of orogenic crust for further research. The ages of S-type magmatism obtained here enhance the idea that the extensional collapse of the Variscan orogen (which has a similar age) is one of the leading processes contributing to the production of voluminous magmatism in NW Iberia. The timing of the S-granites studied here indicates that this particular magmatism occurred in the transition from an extensional-dominated stage (D_2) to a compression-dominated one (D_3). Therefore, melt production/migration likely started during the D_2 extensional stage (i.e., associated with the Pinhel shear zone), but some of the regional structural features associated with their final emplacement in the upper crust were eventually determined by the major D_3 structures that followed (upright folds and strike-slip shear zones) (e.g., Azevedo and Aguado 2013). In this regard, the sheet-like appearance of these granitoids is probably a feature determined by and/or acquired during the waning stages of D_2, whereas their occurrence along the core of upright antiforms and defining elongate massifs parallel to strike-slip shear zones would represent the influence of D_3 during the latest stages of their emplacement (Díez Fernández and Pereira 2016). In this light, Variscan magmatism developed across several stages throughout the evolution of the orogen, and therefore both the ongoing processes leading to melt generation and those contributing to subsequent melt emplacement could be different.

The results presented here for NW Iberia show that the compositional, temporal and spatial evolution of magmatism is distinct from SW Iberia. Remarkably, mantle contributions diminish towards the north and northeast of the Iberian Massif, where extensional syn-orogenic magmatism is slightly younger and is clearly dominated by crustal sources (e.g., Villaseca et al. 1998). In NW Iberia, crustal thickening achieved by the stacking of tectonic nappes and the rejuvenation of reliefs progressed during Tournaisian-Visean and intraorogenic extensional activity had a remarkable development in the Serpukhovian-Bashkirian. The overriding of the Iberian Allochthonous complexes can justify by itself the extensional collapse of the Variscan orogen and the generation of abundant crustal-derived magmatism (Alcock et al. 2015) without an obvious mantle input. However, in SW Iberia something different happened. In the Ossa-Morena and South Portuguese zones, intra-orogenic extension (Simancas et al. 2003; Pereira et al. 2009) started earlier and simultaneously with the emplacement of voluminous Tournaisian-Bashkirian mantle-derived mafic to intermediate (alkaline, calc-alkaline, and metaluminous) and felsic (calc-alkaline and peraluminous) magmatism (Pereira et al. 2015b and references therein). A recently proposed geodynamic model based on terrane correlation between NW and SW Iberia admits that the Carboniferous intraorogenic extension followed the underthrusting of Gondwanan crust towards Laurussia (Díez Fernández et al. 2016). This hypothetical tectonic frame probably favored the creation of a thicker crustal root towards Gondwana (NW Iberia), i.e., a higher mantle topography towards Laurussia that imply a major thermal anomaly in SW Iberia. The upwelling of the asthenosphere was probably responsible for the decompressional melting of the lithospheric mantle which had already been metasomatized by subducted slab-derived melts, leading to the generation of the mafic parental magmas of the calc-alkaline suites in the Ossa-Morena and South Portuguese zones (Pereira et al. 2015b). The underplating of mantle-derived magmas and the intra-orogenic extension created conditions for the anatexis of crustal materials in SW Iberia (Pereira et al. 2009, 2012b), thus leading to the generation and emplacement of voluminous calc-alkaline felsic and mafic plutons at ca. 353–335 Ma (Romeo et al. 2006; Jesus et al. 2007; Pin et al. 2008; Lima et al. 2012; Gladney et al. 2014; Cambeses et al. 2015; Moita et al. 2015; Pereira et al. 2015b), and at ca. 320–317 Ma (Lima et al. 2012). Consequently, once the cohesion of the orogen was lost to its thermal re-equilibrium, the gravitational collapse gained importance through Serpukhovian-Bashkirian times in NW and SW Iberia (Díez Fernández et al. 2016).

Acknowledgements Funding was provided by Fundação para a Ciência e Tecnologia (Portugal) through research project PTDC/GEO–GEO/2446/2012: COMPETE: FCOMP-01-0124-FEDER-029192. Thanks are due to Prof. Neiva and Prof. Corfu for making available the heavy minerals concentrates. The authors thank Klaus Stanek (TU Bergakademie Freiberg) for CL imaging. Reviews by J.B. Brendan, J. Fernández-Suarez and an anonymous reviewer are kindly acknowledged.

References

Alcock JE, Martínez Catalán JR, Rubio Pascual FJ, Montes AD, Díez Fernández R, Gómez Barreiro J, Arenas R, Dias da Silva Í, González Clavijo E (2015) 2-D thermal modeling of HT-LP metamorphism in NW and Central Iberia: implications for Variscan magmatism, rheology of the lithosphere and orogenic evolution. Tectonophysics 657:21–37

Arenas R, Sánchez Martínez S, Díez Fernández R, Gerdes A, Abati J, Fernández-Suárez J, Andonaegui P, González Cuadra P, López Carmona A, Albert R, Fuenlabrada JM, Rubio Pascual FJ (2016) Allochthonous terranes involved in the Variscan suture of NW Iberia: a review of their origin and tectonothermal evolution. Earth Sci Rev 161:140–178

Azevedo M, Aguado B (2013) Origem e Instalação de Granitóides Variscos na Zona Centro-Ibérica. In: Dias R, Araújo A, Terrinha P, Kullberg JC (eds) Geologia de Portugal. Escolar Editora, pp 371–395

Barbero L (1995) Granulite-facies metamorphism in the anatectic complex of Toledo, Spain: late Hercynian tectonic evolution by crustal extension. J Geol Soc 152:365–382

Bea F, Montero P, Molina JE (1999) Mafic precursors, peraluminous granitoids, and late lamprophym in the Avila batholith: a model for the generation of Variscan batholiths in Iberia. J Geol 107:399–419

Bea F, Montero P, Zinger T (2003) The nature, origin, and thermal influence of the granite source layer of Central Iberia. J Geol 111:579–595

Cambeses A, Scarrow JH, Montero P, Molina JF, Moreno JA (2015) SHRIMP U-Pb zircon dating of the Valencia del Ventoso plutonic complex, Ossa-Morena Zone, SW Iberia: early Carboniferous intra-orogenic extension related 'calc-alkaline' magmatism. Gondwana Res. doi:10.1016/j.gr.2014.05.013

Castiñeiras P, Villaseca González C, Barbero González L, Martín Romera C (2008) SHRIMP U-Pb zircon dating of anatexis in high-grade migmatite complexes of Central Spain: implications in the Hercynian evolution of Central Iberia. Int J Earth Sci 97:35–50

Castro A, Patiño Douce AE, Corretgé LG, De La Rosa JD, El-Biad M, El-Hmidi H (1999) Origin of peraluminous granites and granodiorites, Iberian massif, Spain: an experimental test of granite petrogenesis. Contrib Miner Petrol 135:255–276

Castro A, Corretgé LG, De La Rosa J, Enrique P, Martínez FJ, Pascual E, Lago M, Arranz E, Galé C, Fernández C, Donaire T, López S (2002) Paleozoic magmatism. In: Gibbons W, Moreno MT (eds) The geology of spain. Geological Society, London, pp 117–153

Dallmeyer RD, Martínez Catalán JR, Arenas R, Gil Ibarguchi JI, Gutiérrez Alonso G, Farias P, Aller J, Bastida F (1997) Diachronous Variscan tectonothermal activity in the NW Iberian Massif: evidence from $^{40}Ar/^{39}Ar$ dating of regional fabrics. Tectonophysics 277:307–337

Dias da Silva I, Valverde-Vaquero P, González Clavijo E, Díez Montes A, Martínez Catalán JR (2014) Structural and stratigraphical significance of U-Pb ages from the Mora and Saldanha volcanic complexes (NE Portugal, Iberian Variscides). In: Schulmann K, Martínez Catalán JR, Lardeaux JM, Janousek V, Oggiano G (eds) The Variscan orogeny: extent, timescale and the formation of the european crust. Geological Society, London, pp 115–135 **(Special Publications)**

Dias da Silva I, Díez Fernández R, Díez Montes A, González Clavijo E, Foster DA (2016) Magmatic evolution in the N-Gondwana margin related to the opening of the Rheic Ocean—evidence from the Upper Parautochthon of the Galicia-Trás-os-Montes Zone and from the Central Iberian Zone (NW Iberian Massif). Int J Earth Sci 105:1127–1151

Dias G, Leterrier J, Mendes A, Simões PP, Bertrand JM (1998) U-Pb zircon and monazite geochronology of post-collisional Hercynian granitoids from the Central Iberian Zone (Northern Portugal). Lithos 45:349–369

Dias G, Simões PP, Ferreira N, Leterrier J (2002) Mantle and crustal sources in the genesis of Late-Hercynian granitoids (NW Portugal): geochemical and Sr-Nd isotopic constraints. Gondwana Res 5(2):287–305

Dias G, Simões PP, Ferreira N, Leterrier J (2010) Mantle and Crustal Sources in the Genesis of Late-Hercynian Granitoids (NW Portugal): geochemical and Sr-Nd Isotopic Constraints. Gondwana Res 5(2):287–305

Díaz-Alvarado J, Castro A, Fernández C, Moreno-Ventas I (2011) Assessing bulk assimilation in cordierite-bearing granitoids from the Central System Batholith, Spain: experimental, geochemical and geochronological constraints. J Petrol 52:223–256

Díez Balda MA, Martínez Catalán JR, Ayarza P (1995) Syn-collisional extensional collapse parallel to the orogenic trend in a domain of steep tectonics—the Salamanca detachment zone (Central Iberian Zone, Spain). J Struct Geol 17:163–182

Díez Fernández R, Arenas R (2015) The Late Devonian Variscan suture of the Iberian Massif: a correlation of high-pressure belts in NW and SW Iberia. Tectonophysics 654:96–100

Díez Fernández R, Pereira MF (2016) Extensional orogenic collapse captured by strike-slip tectonics: constraints from structural geology and U-Pb geochronology of the Pinhel shear zone (Variscan orogen, Iberian Massif). Tectonophysics 691:290–310

Díez Fernández R, Pereira MF (2017) Strike-slip shear zones of the Iberian Massif: are they coeval? Lithosphere **(in press)**

Díez Fernández R, Martínez Catalán JR, Gómez Barreiro J, Arenas R (2012) Extensional flow during gravitational collapse: a tool for setting plate convergence (Padrón migmatitic dome, Variscan belt, NW Iberia). J Geol 120:83–103

Díez Fernández R, Gómez Barreiro J, Martínez Catalán JR, Ayarza P (2013) Crustal thickening and attenuation as revealed by regional fold interference patterns: ciudad Rodrigo basement area (Salamanca, Spain). J Struct Geol 46:115–128

Díez Fernández R, Arenas R, Pereira MF, Sánchez Martínez S, Albert R, Martín Parra LM, Rubio Pascual FJ, Matas J (2016) Tectonic evolution of Variscan Iberia: gondwana–Laurussia collision revisited. Earth Sci Rev 162:269–292

Escuder Viruete JE, Arenas R, Martínez Catalán JR (1994) Tectonothermal evolution associated with Variscan crustal extension in the Tormes gneiss dome (NW Salamanca, Iberian massif, Spain). Tectonophysics 238:117–138

Escuder Viruete J, Hernáiz Huerta PP, Valverde-Vaquero P, Rodríguez Fernández R, Dunning G (1998) Variscan syncollisional extension in the Iberian Massif: structural, metamorphic and geochronological evidence from the Somosierra sector of the Sierra de Guadarrama (Central Iberian Zone, Spain). Tectonophysics 290:87–109

Farias P, Ordoñez-Casado B, Marcos A, Rubio-Ordoñez A, Fanning CM (2014) U-Pb zircon SHRIMP evidence for Cambrian volcanism in the Schistose Domain within the Galicia-Trás-os-Montes Zone (Variscan Orogen, NW Iberian Peninsula). Geologica Acta 12(3):209–218

Fernández-Suárez J, Dunning GR, Jenner GA, Gutierrez-Alonso G (2000) Variscan collisional magmatism and deformation in NW Iberia: constraints from U-Pb geochronology of granitoids. J Geol Soc 157:565–576

Fernández-Suárez J, Gutierrez-Alonso G, Johnston ST, Jeffries TE, Pastor-Galán D, Jenner GA, Murphy JB (2011) Iberian late-Variscan granitoids: some considerations on crustal sources and the significance of "mantle extraction ages". Lithos 123:121–132

Ferreira N, Sousa MB (1994) Carta Geológica de Portugal, scale 1:50000, Notícia explicativa da Folha 14-B Moimenta da Beira. Instituto Geológico e Mineiro

Ferreira N, Ponce Iglesias, de León M, Noronha F, Ribeiro A, Ribeiro ML (1987) Granitóides da Zona Centro Ibérica e seu enquadramento geodinâmico. In: Bea F, Carnicero A, Gonzalo JC, López-Plaza M, Rodríguez Alonso MD (eds) Geología de los granitoides y rocas asociadas del Macizo Hespérico. Libro Homenaje a L.C. García de Figuerola. Ediciones Rueda, Madrid, pp 37–51

Frei D, Gerdes A (2009) Precise and accurate in situ U-Pb dating of zircon with high sample throughput by automated LA-SF-ICP-MS. Chem Geol 261(3–4):261–270

Gladney ER, Braid JA, Murphy JB, Quesada C, McFarlane CRM (2014) U-Pb geochronology and petrology of the late Paleozoic Gil Marquez pluton: magmatism in the Variscan suture zone, southern Iberia, during continental collision and the amalgamation of Pangea. Int J Earth Sci 103:1433–1451

González Clavijo E, Martínez Catalán JR (2002) Stratigraphic record of preorogenic to synorogenic sedimentation, and tectonic evolution of imbricate thrusts in the Alcañices synform (northwestern Iberian Massif). In: Martínez Catalán JR, Hatcher Jr. RD, Arenas R, Días García F (eds) Variscan appalachian dynamics: the building of the Late Palaeozoic basement. Geological Society of America, pp 17–25

Gutiérrez Marco JC, San Jose MA, Pieren AP (1990) Central Iberian Zone, autochthonous sequences: post-Cambrian Palaeozoic stratigraphy. In: Dallmeyer RD, Martínez García E (eds) Pre-mesozoic geology of Iberia. Springer, Berlin, pp 160–171

Gutiérrez-Alonso G, Fernández-Suárez J, Jeffries TE, Johnston ST, Pastor-Galán D, Murphy JB, Franco MP, Gonzalo JC (2011) Diachronous post-orogenic magmatism within a developing orocline in Iberia, European Variscides. Tectonics 30, TC5008

Jesus A, Munhá J, Mateus A, Tassinari C, Nutman A (2007) The Beja layered gabbroic sequence (Ossa-Morena Zone, Southern Portugal): geochronology and geodynamic implications. Geodin Acta 20:139–157

Julivert M, Fontboté JM, Ribeiro A, Conde LE (1974) Memória explicativa del Mapa Tectónico de la Peninsula Ibérica y Baleares. Scale 1/1000000. Inst Geol Minero España

Lima SM, Corfu F, Neiva AMR, Ramos MF (2012) Dissecting complex magmatic processes: an in-depth U-Pb Study of the Pavia Pluton, Ossa-Morena Zone, Portugal. J Petrol 53(9):1887–1911

Ludwig KR (2001) Isoplot 3.0: a geochronological toolkit for Microsoft excel: special publication N. 4. Berkeley Geochronology Center, Berkeley, p 71

Martínez Catalán JR, Arenas R, Díaz García F, Abati J (1997) Variscan accretionary complex of northwest Iberia: terrane correlation and succession of tectonothermal events. Geology 25:103–1106

Martínez Catalán JR, Arenas R, Díaz García F, Gómez Barreiro J, González Cuadra P, Abati J, Castiñeiras P, Fernández-Suárez J, Sánchez Martínez S, Andonaegui P, González Clavijo E, Díez Montes A, Rubio Pascual FJ, Valle Aguado B (2007) Space and time in the tectonic evolution of the northwestern Iberian Massif. Implications for the Variscan belt. In: Hatcher RD, Carlson MP, Mcbride JH, Martínez Catalán JR (eds) 4-D framework of continental crust. Geological Society of America Memoir, Boulder, pp 403–423

Martínez Catalán JR, Arenas R, Abati J, Sánchez Martínez S, Díaz García F, Fernández-Suárez J, González Cuadra P, Castineiras P, Gómez Barreiro J, Díez Montes A, González Clavijo E, Rubio Pascual FJ, Andonaegui P, Jeffries TE, Alcock JE, Díez Fernández R, López Carmona A (2009) A rootless suture and the loss of the roots of a mountain chain: the Variscan belt of NW Iberia. Comptes Rendus Geosci 341:114–126

Martínez Catalán JR, Rubio Pascual FJ, Díez Montes A, Díez Fernández R, Gómez Barreiro J, Dias da Silva Í, González Clavijo E, Ayarza P, Alcock JE (2014) The late Variscan HT/LP metamorphic event in NW and Central Iberia: relationships to crustal thickening, extension, orocline development and crustal evolution. Geol Soc Lond Spec Publ 405:225–247

Martínez Poyatos D, Gutíerrez-Marco JC, Pardo Alonso MV, Rábano I, Sarmiento G (2004) Zona Centro Ibérica, Dominio del Complejo Esquisto-Grauvaquico, Estratigrafia: La secuencia paleozóica postcámbrica. In: Vera JA (ed) Geología de España. SGE, IGME, pp 81–83

Merino Martínez E, Villaseca C, Orejana D, Pérez-Soba C, Belousova E, Andersen T (2014) Tracing magma sources of three different S-type peraluminous granitoid series by in situ U-Pb geochronology and Hf isotope zircon composition: the Variscan Montes de Toledo batholith (central Spain). Lithos 200–201:273–298

Moita P, Santos JF, Pereira MF, Costa MM, Corfu F (2015) The quartz-dioritic Hospitais intrusion (SW Iberian Massif) and its mafic microgranular enclaves—evidence for mineral clustering. Lithos 224–225:78–100

Neiva AMR, Gomes MEP (2001) Diferentes tipos de granitos e seus processos petrogenéticos: Granitos Hercínicos Portugueses. Memórias da Academia das Ciências de Lisboa XXXIX, pp 53–95

Neiva AMR, Williams IS, Ramos JMF, Gomes MEP, Silva MMVG, Antunes IMHR (2009) Geochemical and isotopic constraints on the petrogenesis of Early Ordovician granodiorite and Variscan two-mica granites from the Gouveia area, central Portugal. Lithos 111:186–202

Neiva AMR, Williams IS, Lima SM, Teixeira RJS (2012) U-Pb and $^{39}Ar/^{40}Ar$ data constraining the ages of the source, emplacement and recrystallization/cooling events from late- to post-D3 Variscan granites of the Gouveia area, central Portugal. Lithos 153:72–83

Noronha F, Ramos JMF, Rebelo JA, Ribeiro A, Ribeiro ML (1978) Essai de corrélation des phases de déformation hercynienne dans le Nord-Ouest péninsulaire. Boletim da Sociedade Geológica de Portugal 21:227–237

Oliveira JT (1992) Carta Geológica de Portugal, Folha Norte, scale 1/500000. Serviços Geológico de Portugal

Orejana D, Villaseca C, Valverde-Vaquero P, Belousova EA, Armstrong RA (2012) U-Pb geochronology and zircon composition of late Variscan S- and I-type granitoids fromthe Spanish Central System. Int J Earth Sci. doi:10.1007/s00531-012-0750-y

Pereira MF (2015) Potential sources of Ediacaran strata of Iberia: a review. Geodin Acta 27:1–14

Pereira MF, Chichorro M, Williams IS, Silva JB, Fernández C, Díaz-Azpíroz M, Apraiz A, Castro A, (2009) Variscan intra-orogenic extensional tectonics in the Ossa-Morena Zone (Évora-Aracena-Lora del Río metamorphic belt, SW Iberian Massif): SHRIMP zircon U-Th-Pb geochronology. Geological Society, London, pp 215–237 (**Special Publications**)

Pereira MF, Linnemann U, Hofmann M, Chichorro M, Sola AR, Medina J, Silva JB (2012a) The provenance of Late Ediacaran and Early Ordovician siliciclastic rocks in the Southwest Central Iberian Zone: constraints from detrital zircon data on northern Gondwana margin evolution during the late Neoproterozoic. Precambr Res 192–195:166–189

Pereira MF, Chichorro M, Silva JB, Ordóñez-Casado B, Lee JKW, Williams IS (2012b) Early Carboniferous wrenching, exhumation of high-grade metamorphic rocks and basin instability in SW Iberia: constraints derived from structural geology and U-Pb and ^{40}Ar-^{39}Ar geochronology. Tectonophysics 558–559:28–44

Pereira I, Dias R, Bento dos Santos T, Mata J (2014) Zona de Cisalhamento de Juzbado-Penalva do Castelo no sector de Figueira de Castelo Rodrigo: implicações para a exumação de rochas metamórficas de alto grau. Comunicações Geológicas 101:289–292

Pereira MF, Castro A, Fernández C (2015a) The inception of a Paleotethyan magmatic arc in Iberia. Geosci Front 6:297–306

Pereira MF, Chichorro M, Moita P, Santos JF, Solá AMR, Williams IS, Silva JB, Armstrong RA (2015b) The multistage crystallization of zircon in calc-alkaline granitoids: U-Pb age constraints on the timing of Variscan tectonic activity in SW Iberia. Int J Earth Sci 104:1167–1183

Pin C, Fonseca PE, Paquette J-L, Castro P, Matte Ph (2008) The ca. 350 Ma Beja Igneous Complex: a record of transcurrent slab break-off in the Southern Iberia Variscan Belt? Tectonophysics 461:356–377

Regêncio Macedo CA (1988) Granitoides, Complexo Xisto-Graiváquico e Ordovícico na região entre Trancoso e Pinhel (Portugal Central): geologia, petrologia, geocronologia. Unpublished PhD thesis, Universidade de Coimbra, Coimbra, p 430

Silva AF, Ribeiro, ML (1991) Carta Geológica de Portugal, scale 1:50000, Notícia explicativa da Folha 15-A Vila Nova de Foz Côa. Serviços Geológicos de Portugal

Ribeiro A, Pereira E, Dias R (1990) Structure in the northwest of the Iberian Peninsula. In: Dallmeyer RD, Martínez García E (eds) Pre-mesozoic geology of Iberia. Springer, Berlin, pp 220–236

Rodríguez-Alonso MD, Peinado M, Lopez-Plaza M, Franco P, Carnicero A, Gonzalo JC (2004) Neoproterozoic-Cambrian synsedimentary magmatism in the Central Iberian Zone (Spain): geology, petrology and geodynamic significance. Int J Earth Sci 93:897–920

Romeo I, Lunar R, Capote R, Quesada C, Dunning GR, Pina R, Ortega L (2006) U-Pb age constraints on Variscan magmatism and Ni-Cu-PGE metallogeny in the Ossa-Morena Zone (SW Iberia). J Geol Soc 163:837–846

Rubio Pascual FJ, Arenas R, Catalán JRM, Fernández LRR, Wijbrans JR (2013) Thickening and exhumation of the Variscan roots in the Iberian Central System: tectonothermal processes and $^{40}Ar/^{39}Ar$ ages. Tectonophysics 587:207–221

San José MA, Pieren AP, Garcia-Hidalgo JF, Vilas L, Herranz P, Pelaez JR, Prejon A (1990) Central Iberian Zone, autochthonous sequences: ante-Ordovician stratigraphy. In: Dallmeyer RD, Martínez García E (eds) Pre-mesozoic geology of Iberia. Springer, Berlin, pp 145–159

Sousa MB, Sequeira, AJD (1989) Carta Geológica de Portugal, scale 1:50000, Notícia explicativa da Folha 10-D Alijó. Serviços Geológicos de Portugal

Silva AF, Ribeiro ML (1994) Carta Geológica de Portugal, scale 1:50000, Notícia explicativa da Folha 15-B Freixo de Espada à Cinta. Instituto Geológico e Mineiro

Simancas JF, Carbonell R, Gonzalez Lodeiro F et al (2003) Crustal structure of the transpressional Variscan orogen of SW Iberia: SW Iberia deep seismic reflection profile (IBERSEIS). Tectonics 22:1062

Simões RP (2000) Instalação, geocronologia e petrogénese de granitóides biotíticos sintectónicos associados ao cisalhamento Vigo-Régua (ZCI, Norte de Portugal). Unpublished PhD thesis, Universidade do Minho, Braga, p 351

Stacey JC, Kramers JD (1975) Approximation of terrestrial lead isotope evolution by a two-stage model. Earth Planet Sci Lett 26(2):207–221

Talavera C, Montero P, Martínez Poyatos D, Williams IS (2012) Ediacaran to Lower Ordovician age for rocks ascribed to the Schist-Graywacke Complex (Iberian Massif, Spain): evidence from detrital zircon SHRIMP U-Pb geochronology. Gondwana Res 22:928–942

Talavera C, Montero P, Bea F, González-Lodeiro F, Whitehouse M (2013) U-Pb zircon geochronology of the Cambro-Ordovician metagranites and metavolcanic rocks of central and NW Iberia. Int J Earth Sci 102:1–23

Teixeira RJS (2008) Mineralogia, petrologia e geoquímica dos granitos e seus encraves da região de Carrazeda de Ansiães. Unpublished PhD thesis, University of Trás-os-Montes e Alto Douro, p 430

Teixeira RJS, Neiva AMR, Gomes MEP, Corfu F (2007) Geoquímica de alguns granitos da região de Carrazeda de Ansiães, Norte de Portugal, e seu enriquecimento em estanho. XV Semana-VI Congresso Ibérico de Geoquímica, Vila Real, pp 101–104

Teixeira RJS, Neiva AMR, Silva PB, Gomes MEP, Andersen T, Ramos JMF (2011) Combined U-Pb geochronology and Lu–Hf isotope systematics by LAM–ICPMS of zircons from granites and metasedimentary rocks of Carrazeda de Ansiães and Sabugal areas, Portugal, to constrain granite sources. Lithos 125:321–334

Ugidos JM (1990) Central Iberian Zone, autochthonous sequences, granites as a paradigm of genetic processes of granitic rocks: I-types vs S-types. In: Dallmeyer RD, Martínez García E (eds) Pre-mesozoic geology of Iberia. Springer, Berlin, pp 189–206

Valle Aguado B, Azevedo MR, Schaltegger U, Martínez Catalán JR, Nolan J (2005) U-Pb zircon and monazite geochronology of Variscan magmatism related to syn-convergence extension in Central Northern Portugal. Lithos 82:169–184

Valverde-Vaquero P, Dunning GR (2000) New U-Pb ages for Early Ordovician magmatism in central Spain. J Geol Soc Lond 157:15–26

Valverde-Vaquero P, Díez-Balda MA, Díez-Montes A, Dörr W, Escuder-Viruete J, González-Clavijo E, Maluski H, Rodríguez-Fernández LR, Rubio F, Villar P (2007) The "hot orogeny: two separate Variscan low-pressure metamorphic events in the Central Iberian Zone. Géol Fr 2:168p

Villaseca C, Herreros V (2000) A sustained felsic magmatic system: the Hercynian granitic batholith of the Spanish Central System. Trans R Soc Edinb Earth Sci 91:207–219

Villaseca C, Barbero L, Rogers G (1998) Crustal origin of Hercynian peraluminous granitic batholiths of Central Spain: petrological, geochemical and isotopic (Sr, Nd) constraints. Lithos 43:55–79

Villaseca C, Downes H, Pin C, Barbero L (1999) Nature and composition of the lower continental crust in Central Spain and the granulite-granite linkage: inferences from granulitic xenoliths. J Petrol 40:1465–1496

Villaseca C, Orejana D, Belousova EA (2012) Recycled metaigneous crustal sources for S- and I-type Variscan granitoids from the Spanish Central System batholith: constraints from Hf isotope zircon composition. Lithos 153:84–93